

# PROCESS, MEASUREMENT, AND ENVIRONMENTAL FLUCTUATION ALL AT ONCE: A NAIVE THEORY-DRIVEN ANALYSIS OF INTRA-INDIVIDUAL DYNAMICS

YONGFU LIAO

August 12, 2023

## 1. INTRODUCTION

3 The surge of ecological momentary assessment (EMA) studies  
in clinical sciences has called for new statistical methods to analyze  
intra-individual (i.e., idiographic) longitudinal data. A variety of  
6 techniques, such as vector autoregressive (VAR) models, have been  
proposed to infer the (Granger) causal relationships between variables  
from such data (for an overview, see Bringmann (2021) and Piccirillo  
9 & Rodebaugh (2019); also see Ryan & Hamaker (2022) for continuous-  
time VAR models). These VAR models are often employed more  
or less as data-driven, theory-free inferential devices, in which the  
12 researchers place no prior assumptions on the dynamical processes  
underlying change and measurement. We note the danger of such  
practices and also raise an often-ignored issue of *relating measurement*  
15 *to theory*. When a measure is assumed to measure *only* the targeted  
construct plus some random noise, the results of an analysis can never  
inform—and lead to further refinements of—the measurement. Since  
18 the validity of the measurement is *given* in the analysis, it cannot be  
touched (Bringmann & Eronen, 2016). We illustrate this through a  
simple theory-driven analysis of change processes, in which the issue  
21 becomes magnified in a longitudinal setting. Through the analysis,  
it is shown that without explicit theoretical assumptions imposing  
constraints on how measurement and change processes might evolve

---

The supplementary analysis documentation and the code for re-producing this study are available at <https://yongfu.name/intra> and <https://github.com/liao961120/intra> respectively.

24 and interact over time, the resulting inferred processes will inevitably  
conflate multiple untraceable sources of variation, obscuring the  
information that could be gained from statistical inference.

27 Specifically, we are pointing to the importance of teasing out pro-  
cess variation from (pure) measurement errors. This is critical since  
change processes are *independent* of the measurement process—if the  
30 fluctuations observed in repeated measures of a process reflect *only* mea-  
surement errors rather than changes in that process, these observed  
decreases or increases will *not* carry over to the process’s future states.  
33 However, complicating this is that measurements are likely *not pure*.  
Instead of singly measuring the process of interest, psychological mea-  
surements are far from perfect that they probably also measure irrelevant  
36 processes to our dismay. Therefore, we are now faced with the confusing  
variation observed in a time series—it could either arise from measure-  
ment errors, changes in the process of interest, changes in the process  
39 of disinterest, or a combination of any of the former.

In this study, we illustrate the above-discussed scenario through sta-  
tistical analyses of simulated data. The context and theory we choose,  
42 as later seen, are deliberately naive and simplified. This allows us to  
provide a simple yet clear demonstration of embedding theoretical as-  
sumptions into tailored statistical analysis. This also paves the way for  
45 further discussion of current practices of EMA data analyses. Implica-  
tions for future research are also discussed.

## 2. WHAT’S IN A MEASURE

48 In the present article, we distinguish between two types of processes  
and measurement errors. The first process type is what the researchers  
are interested in studying. In a clinical setting, this might be a theo-  
51 rized process that leads to improved clinical outcomes during treatment.  
Here, we take *cognitive reappraisal* as an example. The second process  
type is of disinterest to the researchers but nevertheless sneaks into the  
54 measurement. For our current purpose, we assume this process to be a  
state-like process influenced by environmental triggers of stress and any  
potential aversive effects that lower an individual’s *evaluation* of his or  
57 her cognitive reappraisal ability<sup>1</sup>. Note the first process, *cognitive reap-*  
*praisal*, is more of a trait-like, slow-changing construct as compared to  
the second state-like perceptual process. The distinguishing between  
60 state- and trait-like constructs, as shown later, affects how we theorize  
and model the speed of change in these temporal processes.

---

<sup>1</sup>We further elaborate on and justify this treatment in section 3.2.

Finally, the measurement tool in the current context would be a hypothetical cognitive reappraisal scale. As hinted previously, the measurement process inevitably conflates variation from three different sources. The first is the construct it purports to measure, that is, the true, trait-like ability of cognitive reappraisal. The second is the state-like, rapid-changing process reflecting the aversiveness of the surrounding environment. The remaining variation comes from pure measurement errors, which are introduced every time a measurement is made and are independent of the former two processes.

For the sake of simplicity, in the following text, the first process—the true ability of cognitive reappraisal—is termed the *P-process* and given the abbreviation  $P$ ; the second process—the aversive impact of the surrounding on the evaluation of cognitive reappraisal—is termed the *N-process* and abbreviated as  $N$ ; the latent construct measured by the cognitive reappraisal scale, which is a function of both  $P$  and  $N$ , is abbreviated as  $M$ , and  $S$  denotes the realized observations of  $M$ . FIGURE 1 summarises these relationships between the aforementioned variables.

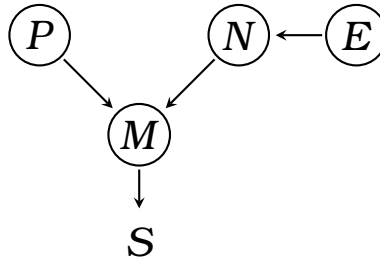


FIGURE 1. Presupposed relationships between *P-process* (cognitive reappraisal,  $P$ ), *N-process* (aversive environmental impact on the evaluation of cognitive reappraisal,  $N$ ), environmental fluctuation ( $E$ ), latent ( $M$ ), and observed ( $S$ ) scores of the cognitive reappraisal scale. The arrows indicate the direction of influences. Circled and open nodes indicate unobserved and observed variables, respectively.

### 3. SIMULATION

In this section, we describe the simulation of each variable in FIGURE 1 and the data-generating process of the full model. Later in section 4, we describe the statistical inference for parameter recovery from the simulated data.

84 To provide some context, consider the scenario in which a hypothet-  
 ical individual, Jane, was receiving CBT for the treatment of mild de-  
 87 pression. During the 49 days between the first and the last session, Jane  
 completed the cognitive reappraisal scale daily to assess her progress. In  
 this hypothetical scenario, the cognitive reappraisal scale is the *only* col-  
 90 lected measure. Later, we relax this assumption and explore the benefits  
 of collecting multiple measures.

In the simulation described below, we will be simulating 98 consecu-  
 tive scores (2 per day) of the cognitive reappraisal scale. Note that the  
 93 observations do not need to be equally spaced for the statistical model to  
 work since we will be using a continuous-time model. This also means  
 that missing data are handled automatically and will not bias inference,  
 96 as long as they are missing at random.

3.1. **Growth of cognitive reappraisal.** We conceptualize cognitive reap-  
 praisal as a skill that gradually develops during the treatment. Therefore,  
 99 cognitive reappraisal is modeled to grow smoothly during the 49-day pe-  
 riod. In particular, the trajectory of the growth is modeled as a logistic  
 function, which can be more informatively expressed as a differential  
 102 equation in (1).

$$\frac{dP}{dt} = rP\left(1 - \frac{P}{K}\right) \quad (1)$$

Equation (1) is known as the logistic population growth, which is  
 often used to model the growth of the population size of a species in  
 105 Biology and Ecology. The left-hand side of Eq. (1),  $\frac{dP}{dt}$ , could be read  
 as the *rate of change* in  $P$ . The right-hand side of Eq. (1) indicates that  
 this rate of change is the product of three components: (a) the intrinsic  
 108 growth rate parameter  $r$ , (b) the current size of  $P$ , and (c) the size of the  
 current  $P$  relative to the carrying capacity parameter  $K$  (Gotelli, 2008).

FIGURE 2 illustrates the trajectories of logistic growth with different  
 111 configurations of  $r$  and  $K$  when the initial size of  $P$  is set to 0.01. Qual-  
 itatively, the intrinsic growth rate  $r$  determines how *fast*, when given  
 a fixed  $K$  and  $P$ ,  $P$  grows. With a larger value of  $r$ ,  $P$  approaches its  
 114 potential maximum more quickly. This is revealed by the three logistic  
 growth curves with a different  $r$  in the left panel of FIGURE 2. On the  
 other hand, the carrying capacity  $K$  represents the upper bound of  $P$ .  
 117 As  $P$  increases and approaches  $K$ , the term  $1 - \frac{P}{K}$  approaches zero, and  
 so does the growth rate  $\frac{dP}{dt}$ . The right panel of FIGURE 2 illustrates three  
 growth curves with a different upper bound  $K$ .

120 Modeling the growth of cognitive reappraisal as a logistic growth  
 curve is an *ideal* assumption, just as a linear growth assumption is in

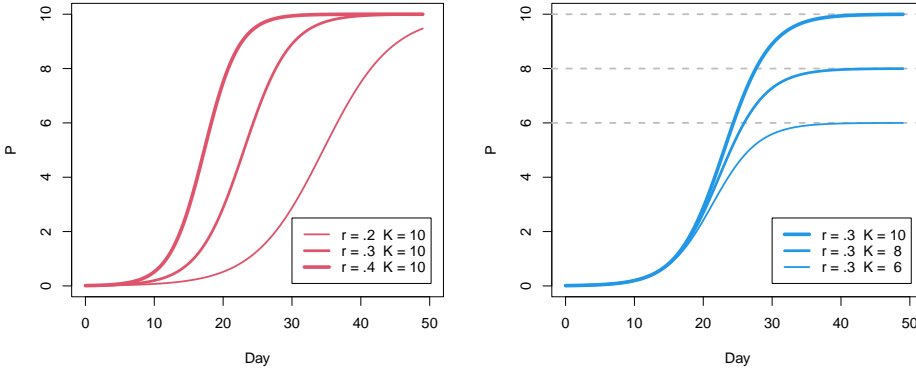


**FIGURE 2.** Logistic growth of  $P$  according to different configurations of  $r$  and  $K$ . The initial value of  $P$  is set to 0.01 for all trajectories.

most models. Logistic growth, however, is arguably more realistic than linear growth in that it models the boundaries of growth ( $0 < P < K$ ) and the deceleration of growth when approaching the boundaries. The shape of the growth over time approximated by a logistic function is thus suitable for modeling a wide range of growth phenomena in nature.

**3.2. Fluctuating environmental impact.** A state-like process is proposed to model the impacts introduced by external stochastic factors on the measurement of cognitive reappraisal. These external impacts are however different from random measurement errors in that they are *continuous and locally dependent*—the impact left on individuals carries on to the immediate and near future but dissipates as time goes by. On the contrary, measurement errors are *discontinued and independent*—measurement errors only occur when measurements are made, and the current magnitude of an error provides no information about any of the future or past measures. The *continuous and local-dependent* property allows the modeling of an individual's experience as a continuum and is based on the idea that, for instance, the stress level experienced by a person currently and 5 seconds later should be nearly identical.

To model this formally, Gaussian processes are used<sup>2</sup>. Gaussian processes allow one to model the covariances between a set of observations

<sup>2</sup>See the supplementary analysis documentation for more details. Also, refer to Wang (2022) and Chap. 4 of McElreath (2020) for an accessible introduction.

as a function of the distances between them. This is illustrated in Equation (2), in which the drawing of a set of time series observations with the help of Gaussian Processes is formulated. The first line in Eq. (2) specifies that  $T$  observations are drawn from a zero mean multivariate normal distribution with a covariance matrix  $\mathbf{K}$ . The essence of Gaussian processes is a covariance function (a.k.a Gaussian process kernel) that defines how the covariance matrix  $\mathbf{K}$  is constructed. This is shown in the second line of Eq. (2), in which  $k_{i,j}$  denotes the entry on the  $i$ th row and  $j$ th column in  $\mathbf{K}$ . The expression on the right-hand side specifies how  $k_{i,j}$  is calculated.  $d_{i,j}^2$  denotes the squared distance between  $N_i$  and  $N_j$ , which is defined as the squared difference between the times at which  $N_i$  and  $N_j$  are recorded.  $\eta$  can be intuitively interpreted as an upper-bound value for all  $k_{i,j}$  (since  $\exp(-\rho d_{i,j}^2) < 1$ ), and  $\rho$  can be thought of as a parameter controlling how quickly  $k_{i,j}$  decays as the distance  $d_{i,j}^2$  increases.

$$\begin{bmatrix} N_1 \\ N_2 \\ \vdots \\ N_T \end{bmatrix} \sim \text{MVNormal}\left(\begin{bmatrix} 0 \\ 0 \\ \vdots \\ 0 \end{bmatrix}, \mathbf{K}\right) \quad (2)$$

$$k_{i,j} = \eta \exp(-\rho d_{i,j}^2)$$

FIGURE 3 sketches four independent draws of time series observations from the same 150-dimensional multivariate normal distribution. This multivariate normal has its covariance matrix  $\mathbf{K}$  generated by a kernel function with parameters  $\eta = 2$  and  $\rho = .15$  and  $150 \times 150$  pairs of distances calculated from the 150 observations sampled at a fixed frequency ( $\frac{150}{49} \approx 3.06$  times per day). Therefore, for each draw of the time series observations in FIGURE 3, the timespan between each pair of adjacent observations is about 7.8 hours ( $24 \text{ hours} \times \frac{49}{150}$ ).

The characteristics of Gaussian processes enable us to naturally model the smooth transition between nearby states and, at the same time, the (nearly) independent fluctuations between distant states. This matches people's daily experiences. For instance, the current stress level is strongly predictive of the stress levels in future hours but is a bad predictor of stress levels weeks later. Likewise, there may be difficult times in life, such as when unpredictable major life events strike that people experience a sudden increased stress level. This experience of a relatively stable period intermitted with rapid fluctuations can also be modeled with Gaussian processes. Take draw 2 in FIGURE 3 for example, the steep dent around day 20 indicates a

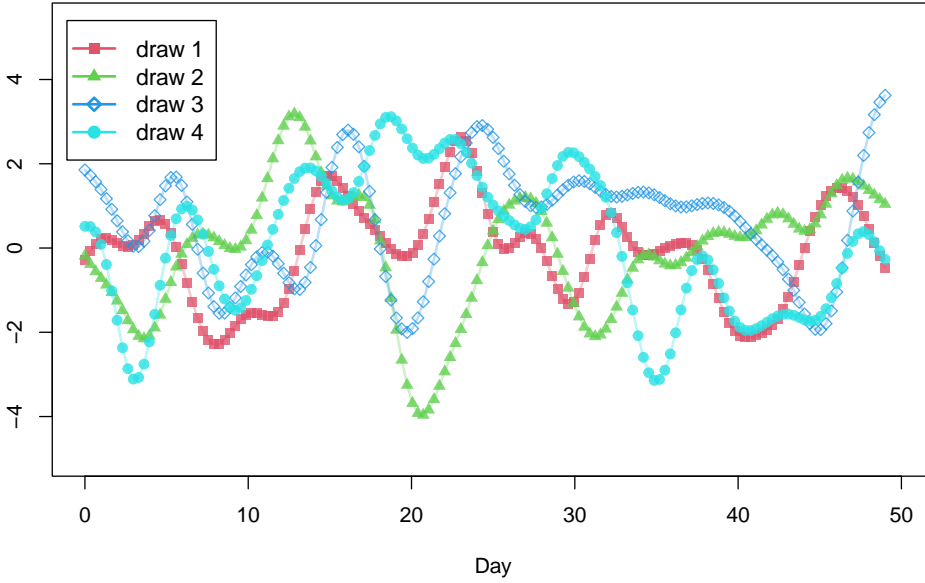


**FIGURE 3.** Four independent sets of time series drawn from a zero mean multivariate normal, whose covariance matrix is generated by a Gaussian process kernel in Eq. (2) with parameters  $\eta = 2$  and  $\rho = .15$ .

period of fast-changing states, whereas the states between day 35 and 45 are relatively stable.

The purpose of modeling the impacts of such experiences is to separate their contribution to the measurement from other sources. This is based on the assumption that psychological measurements partially measure unwanted constructs, which, in turn, is based on the intuition that, say, when a stressed individual is facing challenges one after another, the failure to handle some of these challenges can lower one's judgment of his/her ability. The decreased measurement score thus does not necessarily indicate a measurement error or a drop in one's true ability but may rather be an indicator of environmental aversiveness.

**3.3. Measurement process.** The measurement process conflates the former two processes—the *P-process* and the *N-process*—and adds in some random noise every time a measurement is made. This is formulated in Equation (3).

$$\begin{aligned} P_t^{\text{obs}} &\sim \text{Normal}(M_t, \sigma) \\ M_t &= b [aP_t - (1 - a)N_t] - c \end{aligned} \tag{3}$$

$P_t^{\text{obs}}$  represents the observed score of the cognitive reappraisal scale collected at time  $t$ . The measurement model here assumes that the observed score  $P_t^{\text{obs}}$  distributes normally<sup>3</sup> around the latent score  $M_t$  with the standard deviation of measurement errors being  $\sigma$ . In addition, the latent score  $M_t$  is itself a composite of multiple factors—the cognitive reappraisal skill ( $P_t$ ) and the aversive environmental impact ( $N_t$ ). The parameter  $a$  (constrained between 0 and 1) specifies the contribution of  $P_t$ —relative to  $N_t$ —to  $M_t$ . The parameters  $b$  (scaling factor) and  $c$  (intercept) work together to map the scale of the underlying processes to that of  $M_t$ .

**3.4. Data-generating process.** Gathering the above three processes gives the full data-generating process for our simulation, represented formally in Equation (4). The formulas in Eq. (4) are identical to those in the previous equations except for Eq. (1). Here, Eq. (1) is reexpressed as a forward Euler form in which the computation of  $P$  over time is more straightforwardly conveyed—the immediate next state  $P_{t+\Delta t}$  equals the current state  $P_t$  plus a tiny change  $rP_t(1 - \frac{P_t}{K})\Delta t$ . Iterating this formula, starting with the initial value  $P_0$ , over 49 days results in a collection of  $P$ s over this period.

### Process Model

$$\begin{cases} P_{t=0} = P_0 \\ P_{t+\Delta t} = P_t + rP_t(1 - \frac{P_t}{K})\Delta t \end{cases}$$

$$\begin{bmatrix} N_1 \\ N_2 \\ \vdots \\ N_T \end{bmatrix} \sim \text{MVNormal}(\begin{bmatrix} 0 \\ 0 \\ \vdots \\ 0 \end{bmatrix}, \mathbf{K}) \quad (4)$$

$$k_{i,j} = \eta \exp(-\rho d_{i,j}^2)$$

### Measurement Model

$$P_t^{\text{obs}} \sim \text{Normal}(M_t, \sigma)$$

$$M_t = b [aP_t - (1 - a) N_t] - c$$

<sup>3</sup>A better alternative is to model the  $P_t^{\text{obs}}$  as *ratings*, which would then require a distribution other than the normal to map the latent  $M_t$  to the observed  $P_t^{\text{obs}}$ . For the sake of simplicity, we adopt the normal distribution for modeling measurement errors.



Table 1 lists the parameters and their values for the simulation. The number of observations  $T$  is set to 98, meaning that two observations are simulated for each day. For convenience, the time intervals between consecutive observations are set to be equal. Thus, with  $T$  and a fixed interval between observations, the timestamps for the observations could be determined, which are then used to compute the distances between all pairs of the observations for the Gaussian process kernel.

Table 1: Parameter values for the simulation in Eq (4). The last column specifies the prior distributions assigned to the parameters in the statistical model described in section 4.

Parameter	Coded Name	True Value	Prior
$r$	<code>r</code>	0.30	Beta(1.7, 2)
$K$	<code>K</code>	10.0	Normal(10, 3)
$P_0$	<code>P0</code>	0.01	Normal <sup>+</sup> (0, 0.5)
$\eta$	<code>max_cov</code>	2.00	Normal <sup>+</sup> (0, 3)
$\rho$	<code>rate</code>	0.20	Normal <sup>+</sup> (0, 0.3)
$\sigma$	<code>s1</code>	0.50	Normal <sup>+</sup> (0, 1)
$a$	<code>a1</code>	0.78	Beta(3.8, 2.5)
$b$	<code>b1</code>	0.74	Beta(2, 1)
$c$	<code>c1</code>	3.14	Normal <sup>+</sup> (0, 2)

Running the simulation specified in Eq. (4) with the parameter values in Table 1 gives FIGURE 4. The dashed curves in the figure sketch the trajectories of the *unobserved processes* over time—the gray curve plots the fluctuating environmental impacts on the measurement of cognitive reappraisal ( $N_t$ ), and the smooth red curve plots the growth of the cognitive reappraisal skill ( $P_t$ ). The latent score of the cognitive reappraisal scale ( $M_t$ ), which is a product of the former two processes, is represented as the solid red curve, and the red dots scattering around the curve are the observed scores ( $P_t^{\text{obs}}$ ).

#### 4. INFERENCE

To infer the parameters from the observed time series, a Bayesian statistical model assuming the same data-generating process of the simulation (i.e., Eq. (4)) is constructed and implemented in the probabilistic programming language Stan (Carpenter et al., 2017). A Bayesian model is used here since our data-generating process includes an ordinary differential equation (ODE) to model the nonlinear growth of the P-process. Such ODE-based models are harder to fit within a

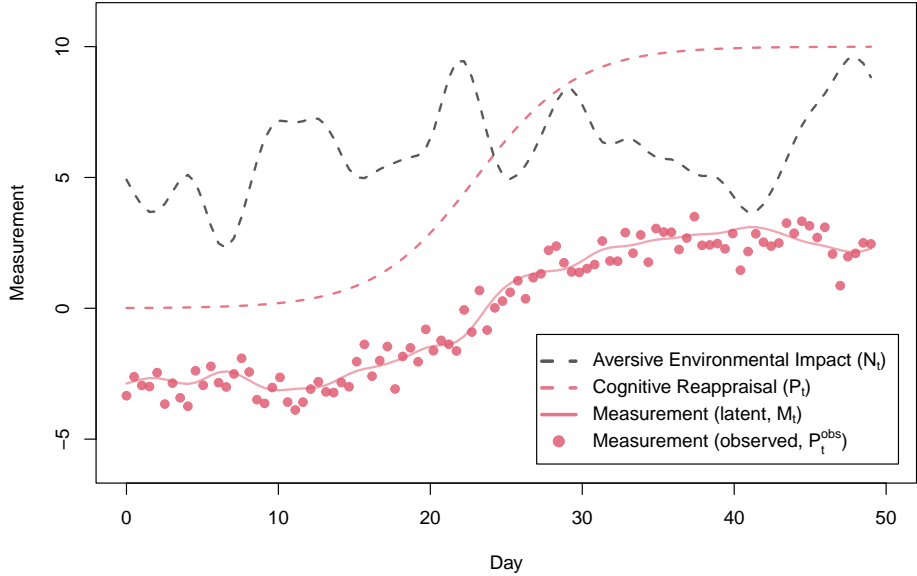


**FIGURE 4.** A run of the simulation specified Eq. (4) with parameter values in Table 1. To avoid cluttering the graph, the grayed dashed curve representing the  $N$ -process is shifted upwards by 5 units (it should be centered at zero originally).

frequentist framework and require specialized software. In addition, Bayesian models are more transparent concerning issues such as identifiability and model convergence. When fitting complex models that include nonlinearity and multiple latent variables, it is nearly impossible to not run into convergence problems. Bayesian models—Stan models in particular—provide valuable information such as MCMC traces and warnings of problematic posterior sampling (e.g., divergent transitions) for diagnosing potential causes of the model’s pathological behaviors.

We code the data-generating process in Eq. (4) into our statistical model and assign weakly informative prior distributions to the parameters. The last column in Table 1 lists the assigned priors. The superscript “+” on some of the priors indicates that they are restricted to positive values.

**4.1. More observations, better inference?** In section 3, we simulated 98 time series observations. To test the ability of our statistical model under different conditions, we first use *half* of the observations to fit the model and inspect how well the parameters are recovered. We then

include all the 98 observations to see how the inference benefits from more repeated measures.

Although adding more data does improve the recovery of parameters, the recovery is far from satisfying—the posterior predictions of the N-process do not converge to the true values, thus failing to separate the sources of variation in the time series. This is even true after we attempted lowering the variation in the measurement error and refitted the model. In fact, lowering the measurement error leads to pathological behaviors in the MCMC samplers, which signals that the model may have identifiability issues<sup>4</sup>. The first 3 panels (the panels with titles beginning with “Model 1”) in FIGURE 5 plot the predictions computed from 20 draws of the posterior samples against the true (i.e., simulated) values. As shown in the plots on the first row, increasing the sample size from 49 to 98 does not help the thin gray lines (20 draws of the N-process posterior predictions) converge to the thick gray line (the true N-process). Although the lower left plot seems to indicate a better inference when the model is fitted with data from more accurate measures, the inference cannot be trusted due to the aforementioned pathologies of the posterior sampling. In sum, including more repeated measures, and even more *accurate* repeated measures, brings about a limited benefit to the inference of the latent dynamics.

**4.2. The power of parallel measurement.** As illustrated in the previous section, with only a single time series, the model cannot reliably recover the latent dynamics that give rise to the observed data, no matter the amount or accuracy of the measure. We therefore explore the potential of improving inference by adding measures *parallel* to the existing one. We hypothesize that with more than one type of measure, and given that all measures at least capture part of the N-process, the model would then be better at distinguishing the sources of variation since it can now leverage the fact that measurement errors are independent across measure types, but the variations introduced by the N-process are shared across.

To explore such a possibility, we modify the simulation to include another time series along with the original one. This is formally expressed as the expanded measurement model in (5):

---

<sup>4</sup>See the *Inference* section of the supplementary analysis documentation.

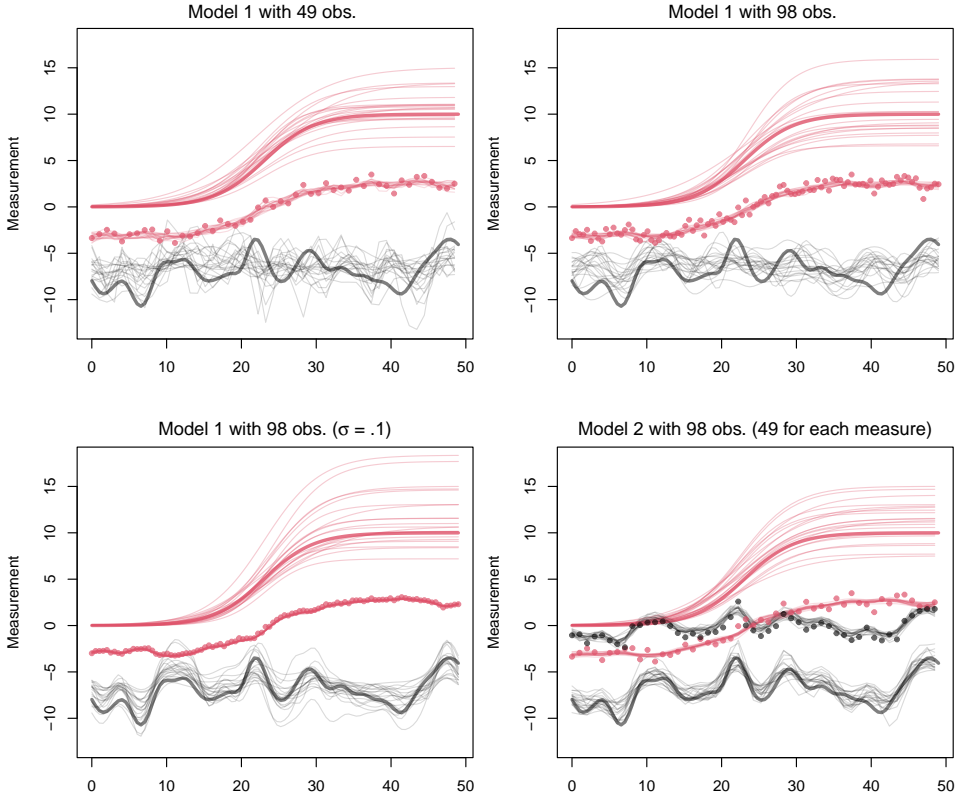


**FIGURE 5.** Posterior predictions generated from the fitted models. Model 1 is fitted to a single set of time series observations that has information about the P-process and the N-process. Model 2 is fitted to the same observations and another set that has information about the N-process. Each panel represents a fit with different configurations, as indicated by the plot titles. The thick red and black curves plot the trajectory of the true P- and N-processes respectively. The 20 thin curves scattering around a thick line are a set of 20 predictions computed from 20 draws of posterior samples. For the measurement, the red and black dots plot the time series observations, and the densely distributed curves underneath them are the posterior predictions of their latent scores. Note that to avoid cluttering the plots, the originally zero-centered black curves (the true and estimated N-process) are shifted downwards by 8 units. Otherwise, the thick black curves should perfectly match the dashed gray line in FIGURE 4.

$$\begin{aligned}
P_t^{\text{obs}} &\sim \text{Normal}(M_t^1, \sigma_1) \\
M_t^1 &= b [a_1 P_t - (1 - a_1) N_t] - c_1 \\
N_t^{\text{obs}} &\sim \text{Normal}(M_t^2, \sigma_2) \\
M_t^2 &= a_2 N_t - c_2
\end{aligned} \tag{5}$$

The first two lines of Eq. (5) are identical to those in Eq. (3) except for the indices added to distinguish them from the parameters of the new measure. The model for the newly added measure is shown in the remaining lines of Eq. (5). Here, the parameter  $a_2$  specifies the contribution of the N-process to the latent score  $M_t^2$ . Together with the intercept  $c_2$  and the standard deviation of the measurement error  $\sigma_2$ ,  $a_2$  maps the N-process to the observed scores  $N_t^{\text{obs}}$ .

The parameters of the extended simulation have values identical to the original simulation. For newly added parameters, their values are set to  $a_2 = 0.6$ ,  $c_2 = 0$ , and  $\sigma_2 = 0.5$ . Likewise, the statistical model is expanded to incorporate the new measurement model. The new parameters are assigned the priors listed below:

$$\begin{aligned}
a_2 &\sim \text{Beta}(3, 3) \\
c_2 &\sim \text{Normal}(0, 1) \\
\sigma_2 &\sim \text{Normal}(0, 1)
\end{aligned}$$

Refitting the extended model with two sets of time series observations confirms our reasoning. The model now greatly improves in separating the N-process from measurement errors and better recovers the true variation of the environmental impact, as shown in the lower right panel of FIGURE 5.

## 5. DISCUSSION

This article has shown what could be gained from explicating the processes underlying measurement. Specifically, a theory of individuals' cognitive reappraisal growth and a theory of stochastic environmental impacts enables the construction of a principled statistical analysis to tease out relevant latent processes from data. It also provides guidance on subsequent treatments when the statistical analysis *fails* to recover the processes. These treatments are by no means intuitive and cannot be deduced through *verbal reasoning* alone—simply including more observations does not help even when measurement error is low. This

conclusion is only reachable by iterative simulation and statistical modeling that systematically explore the logical consequences of modifying the theory. In short, without a concrete, and ideally, *formalized* theory in *quantitative* analysis to provide guidance, an analysis is likely to take us nowhere beyond vagueness.

A theory-driven analysis also has the virtue of informing research planning. In addition to telling us what can be achieved through statistical analysis, the unambiguous nature of formalized theory also points out what *cannot* be answered by the current level of knowledge. Given the intertwined statuses of theory, measurement, and data and the inherent difficulty psychological measurements face, this theory-driven perspective of quantitative analysis also hints at potential directions when stuck in the midst of complexity. We briefly discuss related issues in the following sections.

**5.1. What are we measuring?** Validity has always been a fundamental issue for psychological measurements. To validate a new measurement, many procedures are often used to provide different sources of validity evidence such as criterion-referenced validity, convergent and discriminant validity, internal consistency, etc. These procedures, however, are nearly always employed in a cross-sectional manner. Thus, even for a well-validated scale, we do not know how the measured construct behaves over time when repeated measures are collected<sup>5</sup>. Indeed, it is reasonable to assume the construct being measured is actually a *mixture* of multiple processes, in which at least some of them are unrelated to the target construct the scale aims to measure. When cross-sectionally applying the scale *once*, this might not pose a problem provided that the processes unrelated to the target construct are *independent across individuals* such that they can be safely treated as measurement errors. However, when the scale is used longitudinally, and when the (latent) score of the scale is taken to directly represent the target construct, it may obscure the target construct's true functional relationship with time.

Taking our example in this article, a *skill set* (cognitive reappraisal) is theorized to *only grow* during a period of learning/training (psychotherapy). Together with another theory of fluctuating environmental impact on skill measurement, this allows us to explain the phenomenon of temporary high or low scores occurring in batches in intensive longitudinal

---

<sup>5</sup>Repeated measures are sometimes collected for calculating test-retest reliability, but note that the focus is on the reliability of *the scale*, not the *change* of the measured construct over time.

data. This phenomenon is difficult to explain if we simply take the measurement score as the skill level—the temporary drops or rises of the skill can at best be treated as measurement errors, but since measurement errors are supposedly independent across measurement occasions, how do we explain the stark correlations between nearby scores?

From this perspective, it becomes apparent that measurement and theorizing are intertwined. Even if a measurement scale is well-established from previous studies, we have to be careful not to treat the latent score as the theoretical construct itself and base our reasoning on it, particularly in a longitudinal setting. The difficulty we face in applying established measurements longitudinally also indicates how little we know about the target constructs of interest. The tools and procedures often applied for validating a new measurement provide no information about how a target construct changes over time. Indeed, the longitudinal change of a target construct is a *critical* source of validity evidence that is rarely examined seriously.

**5.2. Issues of timescale.** Longitudinal modeling unavoidably raises issues of time. One of them is that the processes driving the observed time series may act at different time scales. Without some understanding or theorizing of the latent process dynamics, it would be impossible to separate and make inferences about such processes. For instance, in our preliminary illustration, the  $P$ -process, the  $N$ -process, and the measurement process are assumed to operate at a slow, a fast, and an instant timescale respectively, as labeled on the arrows in FIGURE 6. The change in  $P$  is assumed to be driven by therapy  $T$ , which occurs at the slowest timescale among all the processes.  $N$ , on the other hand, changes faster as the result of external environmental fluctuations  $E$ . Finally, all arrows pointing to and out from the latent measurement score  $M$  operate at the fastest timescale as they happen within minutes or even seconds when a measurement is made. The measurement process could thus be considered to occur *instantly* compared to the former two processes.

Now consider a potential influence that  $P$  may have on  $N$  in the long run, as shown in the dashed arrow pointing from  $P$  to  $N$ . Specifically, this relationship intends to model the idea that cognitive reappraisal moderates the aversive impact of the environment on the individual, which is one of the theoretical reasons why developing better reappraisal skills leads to improved outcomes. How, then, could we extend our previous model to incorporate this relationship? Holding on to the timescales at which the processes operate can guide us through. Since now two independent processes are driving  $N$  at different timescales, we need to *simultaneously* model the short- and long-term change in  $N$ .

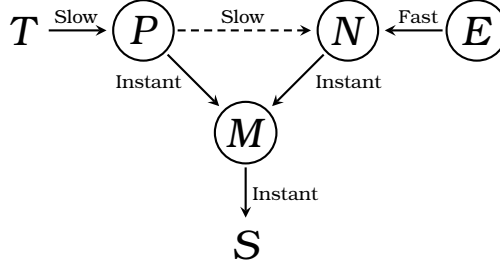


FIGURE 6. Timescales at which the P-process, the N-process, and the measurement process operate in our theory-driven analysis.

390 This can be achieved by linking the influence of  $P$  on  $N$  to the means of  
 the multivariate normal from which  $N$  is drawn, as shown in the modi-  
 393 fied model (4.1).  $P^1, P^2, \dots, P^T$  are values of  $P$  at the times corresponding  
 to  $N_1, N_2, \dots, N_T$ . The resulting effect of (4.1) is visualized in FIGURE 7.

$$\begin{cases} P_{t=0} = P_0 \\ P_{t+\Delta t} = P_t + rP_t(1 - \frac{P_t}{K})\Delta t \end{cases}$$

$$\begin{bmatrix} N_1 \\ N_2 \\ \vdots \\ N_T \end{bmatrix} \sim \text{MVNormal}(-\gamma \begin{bmatrix} P^1 \\ P^2 \\ \vdots \\ P^T \end{bmatrix}, \mathbf{K}) \quad (4.1)$$

$$k_{ij} = \eta \exp(-\rho d_{ij}^2)$$

Knowing at which timescales are the latent processes operating is not  
 only important for constructing statistical models but also necessary in-  
 396 formation for data collection—how frequently should observations be  
 collected to enable valid analyses? In studies applying VAR models<sup>6</sup>,  
 theory-irrelevant reasons such as the amount of data needed for the  
 399 models to converge and the frequency of prompts acceptable for the par-  
 ticipants are sometimes used for determining the sampling rate. This is  
 dangerous if the (theoretical) timescales at which the processes operate  
 402 are not cautiously considered. Ignoring the timescale results in uninter-  
 pretable networks at best and completely misleading ones at worst.

<sup>6</sup>See Ong, Hayes, & Hofmann (2022) and Burger et al. (2021) for at-  
 tempts to derive individualized networks with VAR models to facilitate  
 case conceptualization.



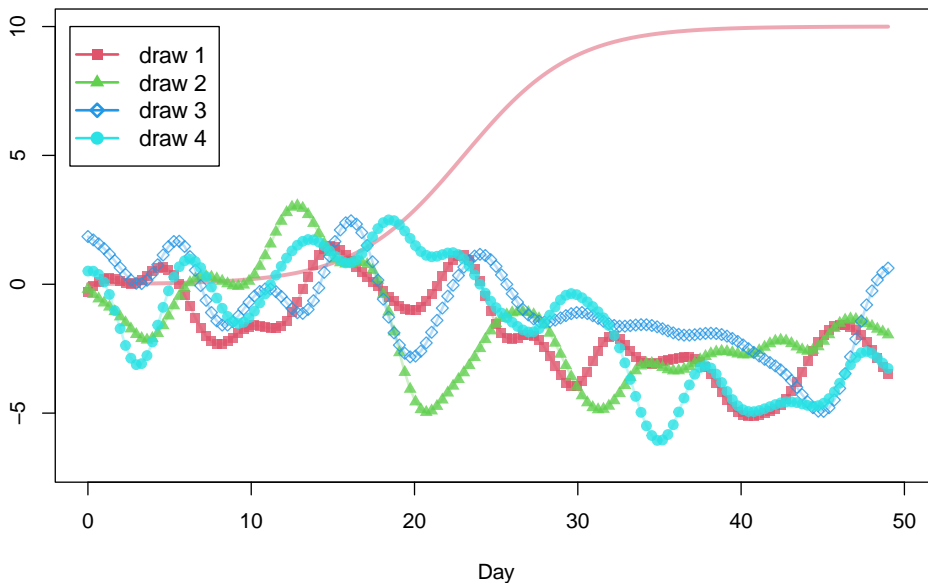


**FIGURE 7.** Reproduction of FIGURE 3 with the added influence of  $P$  on  $N$  over time. The parameters for the growth of  $P$  are  $r = .3, P_0 = .01, K = 10$ . The scaling parameter  $\gamma$  for the influence of  $P$  on the multivariate normal means is set to  $.3$ , and the parameters for the Gaussian kernel  $\eta$  and  $\rho$  are identical to those set for generating FIGURE 3.

To see why, consider a hypothetical example that two groups of researchers wish to study the relationship between lunch and blood sugar levels (suppose they do not know the impact of insulin on blood sugar levels). The first group measured blood sugar 30 minutes after lunch, and the second group measured it 2 hours after lunch. Since blood sugar level first rises and then returns to the homeostatic level in about 2 hours, the first group may conclude that lunch *increases* blood sugar level whereas the second group may end up inferring that lunch has *no* impact on (when the meal is starch-rich), or even *decreases* (when the meal is sucrose-rich), blood sugar level (see Daly et al. (1998), FIGURE 2).

This toy example of blood sugar dynamics illustrates that simply establishing the temporal sequence of events does not automatically license valid causal inference. It also highlights that relationships between variables and time are often nonlinear, and being mindless of the timescale hides this. But this by no means indicates that being aware of the timescale fixes all problems. How the latent processes driving the observed phenomena interact matters even more. Indeed, “Does lunch

change blood sugar level and if so, in which direction?” is arguably a misplaced question. A better approach might be to first establish the functional relationship between blood sugar level and time, after which it is possible to theorize and search for processes that give rise to the observed curve. The blood sugar example also makes clear the importance of observing at the *correct timing*—although it is obvious in such a setting that blood sugar level should be measured *after a meal*, in EMA studies where the time series is usually analyzed as a whole with VAR models, no special attention is paid to such important events. Instead, they are treated *homogeneously* and modeled as random forces that drive the time series away from its equilibrium. Whether this approach is justifiable is related to the issue of *open* and *closed* systems, which we turn to next.

**5.3. Open vs. closed system.** A closed system is a system in which the processes within are unaffected by external forces. An open system, on the other hand, is subject to influences from the outside. Taking the previous blood sugar example, the system that regulates blood sugar can be regarded as an *open* system—the food intake leads to a heightened blood sugar level, which then stimulates the secretion of insulin to drive the blood sugar level back to homeostasis. Note, however, that within a *restricted* time window, it is possible to treat an open system as a closed one—once food is consumed, that is, when external forces are exerted, subsequent physiological responses for blood sugar regulations are irrelevant to the external factors. In other words, in this restricted time window, external forces are controlled for and do not perturb the system, thus it is fine to treat the system as closed.

Most VAR models in the literature model the whole time series as an open system. Specifically, the multivariate time series is modeled as a system of stochastic differential or difference equations. The time series is assumed to be *stationary* (i.e., no trending) and fluctuates randomly around the equilibrium. These random fluctuations, represented through the stochastic components of the equations, are used to model external perturbations pushing the system *away from* its equilibrium. The non-stochastic components of the equations model the driving of the system *back to* equilibrium when perturbed by external forces (Ryan & Hamaker, 2022). Since external perturbations are treated identically as random noise, these models essentially *homogenize* the whole time series—no matter the causes or magnitude of the perturbations, the system is assumed to move back to equilibrium similarly, according to the governing equations.

To provide some context, let's take as an example theories of a "vicious cycle" often used to explain Panic Disorder. Borrowing the terminology from Robinaugh et al. (2019), a simplified hypothesis for the vicious cycle is given as follows: heightened physiological arousal ( $A$ ) raises perceived threat ( $T$ ), which in turn leads to even higher physiological arousal ( $A$ ) and perceived threat, resulting in a positive-feedback loop between physiological arousal and perceived threat. A clinician might want to see if this vicious cycle can be shown empirically with data. Without further elaborating on the theory, however, an EMA study is planned to collect the measures of  $A$  and  $T$  quite densely—once every hour when awake for over 2 months—to infer a network of relationships among these variables. What can we learn from this empirical network? If the hypothesized network of relationships indeed exists and is *robust across situations* such that, for instance, heightened perceived threat leads to higher physiological arousal (and vice versa) *consistently under different situations*, the VAR model would be able to correctly infer the network. However, given that such robust phenomena across situations are rarely found at the behavioral level, the inferred network likely conflates multiple *different* response patterns, leading to an unreliable network whose implications are unclear. Therefore, whether the empirical and the hypothesized networks match or not may not be very informative here, due to a lack of correspondence between statistical analysis and theory—the VAR models are designed to analyze time series data generated from a *homogeneous open* system, whereas the theorized relationships are implicitly conceptualized to operate within a very *specific* situation, which may be more appropriately modeled as a closed system (i.e., within this system, such as when in a crowded theater, (the stimulus of) heightened arousal is *given*, which then triggers subsequent theorized behaviors).

To connect such a theory to data, it is necessary to either locate the *relevant* time windows in which the theorized cascades of behaviors are expected to happen or directly model the *heterogeneity* of the time series<sup>7</sup>, provided that the time series data already has the required resolution. No matter the approach though, it becomes instantly clear that the empirical data needed for validating the theory is extremely hard to collect in the current example. Panic attacks come and go relatively quickly, usually within minutes. Relevant repeated observations need to be collected within these short time windows to match the resolution of the theory. It is unclear how this could be achieved, particularly

---

<sup>7</sup>See e.g., Robinaugh et al. (2019) in which *context* is explicated in their model.

when individuals are required to actively respond to items in such a short period.

**5.4. How to proceed?** A deeper consideration of theories along with their relations with statistical analysis, measurement, and data makes clear that time series analysis of EMA data has a rather shaky foundation. The development of more advanced statistical models is unlikely to provide fixes as the core difficulty lies in collecting data suitable for answering the right questions. The difficulty is twofold.

First, the complexity of human behaviors in the first place makes it extremely hard to even establish phenomena that are robust and reliable (Eronen & Bringmann, 2021). Nonrobust phenomena, in turn, weakens the foundation of theory building, and verbal theories constructed from these phenomena are only vague at best. Finally, the vagueness in theories feeds back to the observation process—a vague theory loses its ability to direct us to the right places looking for answers. We may therefore end up looking for the key under the lamppost, basing our inference on misplaced data.

A possible first step for fixing this is to admit we know too little to conduct quantitative *inferential* studies. A high-quality quantitative study that aims at inferring variable relationships with statistical models requires a strong theoretical foundation, as illustrated throughout the article. Without a strong and explicit theory driving statistical analysis, the results from the analysis will be hard to interpret at best and misleading at worst.

Admitting our limited knowledge allows us to arrive at a logical next step—to establish robust phenomena. Within the context of EMA studies for instance, this may be facilitated with the help of passive measures (e.g., skin conductance, heart rate, blood oxygen level, GPS coordinate, etc.) that could be continuously collected without needing active responses from the participants. Along with other traditional active EMA measures (i.e., responses to items), these data could be fed to purely data-driven machine-learning (ML) algorithms aiming at prediction instead of inference. The goal is to hope that ML algorithms will squeeze out whatever useful information from the multivariate time series to allow the detection of critical time windows informative for further investigation. For instance, with active measures of emotional states acting as the labeling data for ML algorithms, the algorithms may be able to learn subtle patterns contained in other (passive) measures that can reliably predict or forecast, say, rapid emotional shifts. Being able to accurately and reliably predict such events is preliminary evidence that some phenomena exist. Though very little is known about

the nature of the phenomena, at least it is now clearer where we should look at.

Once zoomed in on the relevant locations where the phenomena of interest occur, we are in a better position to deal with harder questions. For instance, we can try to improve the measurement by asking how the measured scores change temporally, theorizing potential processes influencing the measurement, and considering the potential of combining multiple measures to help deal with the imperfect and noisy nature of psychological measurements. These attempts may not only lead to improvements in measurement. Indeed, measurement is *part of* the theory and should be refined hand in hand with the advancement of knowledge (Bringmann & Eronen, 2016).

In practice, the above attempts may all fail. After all, it is likely that at least some rapid-changing phenomena do not leave reliable traces in passive measures that could be monitored continuously. Given this difficult situation, it may be better to let go of the fixation on “quantitative” analysis. Indeed, in practical clinical work, qualitative judgments inform treatment planning much more than quantitative assessments. There is no reason why these kinds of qualitative analyses cannot be employed in a temporarily fine-grained manner. Voice recording along with highly accurate automated audio transcription technologies (e.g., Radford et al., 2022) have lowered the barrier for such qualitative data collection. Gathering qualitative data in such finer-grained details can better deal with reporting and recall biases and might reveal properties that are not visible or apparent in traditional therapy sessions.

## 6. REFERENCES

- Bringmann, L. F. (2021). Person-specific networks in psychopathology: Past, present, and future. *Psychopathology*, 41, 59–64. <https://doi.org/10.1016/j.copsyc.2021.03.004>
- Bringmann, L. F., & Eronen, M. I. (2016). Heating up the measurement debate: What psychologists can learn from the history of physics. *Theory & Psychology*, 26(1), 27–43. <https://doi.org/10.1177/0959354315617253>
- Burger, J., Epskamp, S., van der Veen, D. C., Dablander, F., Schoevers, R. A., Fried, E. I., & Riese, H. (2021). *A clinical PREMISE for personalized models: Towards a formal integration of case formulations and statistical networks*. PsyArXiv. <https://doi.org/10.31234/osf.io/bdrs7>
- Carpenter, B., Gelman, A., Hoffman, M. D., Lee, D., Goodrich, B., Betancourt, M., ... Riddell, A. (2017). Stan: A Probabilistic Programming Language. *Journal of Statistical Software*, 76, 1. <https://doi.org/10.18637/jss.v076.i01>

- Daly, M., Vale, C., Walker, M., Littlefield, A., Alberti, K., & Mathers, J. (1998). Acute effects on insulin sensitivity and diurnal metabolic profiles of a high-sucrose compared with a high-starch diet. *The American Journal of Clinical Nutrition*, 67(6), 1186–1196. <https://doi.org/10.1093/ajcn/67.6.1186>
- Eronen, M. I., & Bringmann, L. F. (2021). The Theory Crisis in Psychology: How to Move Forward. *Perspectives on Psychological Science*, 16(4), 779–788. <https://doi.org/10.1177/1745691620970586>
- Gotelli, N. J. (2008). *A primer of ecology* (4th ed.). Sinauer Associates.
- McElreath, R. (2020). *Statistical rethinking: A Bayesian course with examples in R and Stan* (2nd ed.). Chapman & Hall/CRC.
- Ong, C. W., Hayes, S. C., & Hofmann, S. G. (2022). A process-based approach to cognitive behavioral therapy: A theory-based case illustration. *Frontiers in Psychology*, 13. <https://doi.org/10.3389/fpsyg.2022.1002849>
- Piccirillo, M. L., & Rodebaugh, T. L. (2019). Foundations of idiographic methods in psychology and applications for psychotherapy. *Clinical Psychology Review*, 71, 90–100. <https://doi.org/10.1016/j.cpr.2019.01.002>
- Radford, A., Kim, J. W., Xu, T., Brockman, G., McLeavey, C., & Sutskever, I. (2022). *Robust speech recognition via large-scale weak supervision*. Retrieved from <https://arxiv.org/abs/2212.04356>
- Robinaugh, D., Haslbeck, J. M. B., Waldorp, L., Kossakowski, J. J., Fried, E. I., Millner, A., ... al., et. (2019). *Advancing the network theory of mental disorders: A computational model of panic disorder*. PsyArXiv. <https://doi.org/10.31234/osf.io/km37w>
- Ryan, O., & Hamaker, E. L. (2022). Time to Intervene: A Continuous-Time Approach to Network Analysis and Centrality. *Psychometrika*, 87(1), 214–252. <https://doi.org/10.1007/s11336-021-09767-0>
- Wang, J. (2022). *An intuitive tutorial to gaussian processes regression*. Retrieved from <https://arxiv.org/abs/2009.10862>